Available online at www.sciencedirect.com

SCIENCE DIRECT®

Journal of Molecular Catalysis A: Chemical 206 (2003) 419–428

JOURNAL OF MOLECULAR CATALYSIS A: CHEMICAL

www.elsevier.com/locate/molcata

Photocatalytic activity and recycle application of titanium dioxide sol for X-3B photodegradation

Yibing Xie*, Chunwei Yuan[1]

Key Laboratory of Molecular & Biomolecular Electronics (Southeast University), Ministry of Education, Nanjing 210096, China

Received 23 March 2003; received in revised form 31 May 2003; accepted 11 June 2003

Abstract

In this paper, TiO_2 sol was prepared by chemical coprecipitation–peptization method. XRD pattern shows that TiO_2 sol particles without calcination treatment had anatase crystal structure. The particle size distribution (PSD) analysis shows that TiO_2 sol particles had narrow distribution characterization with a mean size of 21 nm, which was in good agreement with analytical result by AFM (25 nm). A novel hydrosol reaction system was applied to process X-3B photodegradation reaction under visible light illumination. The results demonstrate that TiO_2 sol nanoparticles have better interfacial adsorption capability and higher photoactivity than P25 TiO_2 in suspension system, which was ascribed to the characteristics of better dispersion, less aggregation of composite TiO_2 sol nanoparticles in the aqueous medium. By adjusting the pH value of hydrosol system, TiO_2 sol nanoparticles can be effectively separated from X-3B/TiO_2 hydrosol reaction system and dispersed again into aqueous solution to form sol system. This TiO_2 sol photocatalyst can be applied to recycle use for many times while keeping high photoactivity on X-3B degradation reaction.

Keywords: TiO_2; Sol; Photocatalytic activity; Photosensitization; Recycle use

1. Introduction

Heterogeneous photocatalysis, as a promising advanced oxidization technology, has attracted much attention in the past two decades due to its potential applications in air clean-up and water purification. Titanium dioxide (TiO_2) nanocrystallites have been wide studied due to its remarkable photoactivity to degrade various organic pollutants [1–3]. However, prior to practical application on the industrial scale, many problems need to solve about TiO_2 photocatalysis, such as low photocatalytic efficiency and narrow spectrum responsive range (excitation wavelength <388 nm).

Generally, titania photocatalysis mainly involves two kinds of reaction system.

1. *Suspension system*: Ultrafine TiO_2 powder was dispersed in water.

   Although high photoreaction interfacial area was obtained between reactants and TiO_2 particles, it was big problem how to effectively separate TiO_2 nanoparticles from aqueous solution in order to reuse TiO_2 catalyst.
2. *Immobilization system*: TiO_2 nanoparticles were loaded on the various support.

   This reaction system bypassed the separation step of TiO_2 particles from aqueous solution. However, the photocatalytic efficiency greatly decreased

* Corresponding author. Tel.: +86-25-3791513; fax: +86-25-3609650.
E-mail address: ybxie@seu.edu.cn (Y. Xie).
[1] Co-corresponding author.

1381-1169/$ – see front matter © 2003 Elsevier B.V. All rights reserved.
doi:10.1016/S1381-1169(03)00454-0

because of low reaction interfacial area between TiO_2 film and reactants in aqueous solution.

Another research area was how to expand spectrum responsive range from ultraviolet to visible light and realized solar decontamination of TiO_2 photocatalysis. Many methods were attempted such as organic molecule sensitization and transition metals doping. Some sensitized effect of semiconductor TiO_2 were obtained in visible light range, but there still exist some key problems such as chemical stability of photosensitizer and uncertain effects of metal ion dopants [4–6].

In this paper, TiO_2 sol was prepared by chemical coprecipitation–peptization method. The novel hydrosol reaction system was established, which integrated the advantages of suspension and immobilization reaction system (high photocatalytic efficiency and feasible separation of photocatalysts for recycle use). TiO_2 sol was applied as a useful photocatalyst, and photocatalytic reaction was carried out in hydrosol system to degrade reactive brilliant dyes X-3B. The separation and recycle use of TiO_2 sol were also investigated by adjusting the pH value of aqueous solution. Photocatalytic reaction driven by visible light was applied to X-3B/TiO_2 sol system just by taking advantage of the dye absorption in visible light range.

2. Experimental

2.1. Materials

Titanium dioxide (TiO_2) powder sample used in the experiment was commercial Degussa P25 with 80% anatase, 20% rutile and BET area of ca. $50\,m^2\,g^{-1}$, which was produced by the Degussa AG Company in Germany. Titanium tetrachloride ($TiCl_4$) was pure reagent grade and obtained from J&K China Chemical Ltd. Ammonium hydroxide (NH_4OH), nitric acid (HNO_3), hydrochloric acid (HCl) and other chemicals were analytical reagent grade quality and all obtained from Shanghai reagent company. The high purity water used in the experiment was double distilled and then purified with the Milli-Q system. The substrate of X-3B dye was obtained from Shanghai Dyestuff Chemical Plant and used without further purification. Fig. 1 displays the structure of reactive brilliant red dye X-3B.

2.2. Preparation of titania sol

TiO_2 sol was prepared by chemical coprecipitation–peptization method. Firstly, 50 ml $TiCl_4$ precursor was diluted and hydrolyzed with 100 ml deionized distilled frozen water (0 °C) under vigorous stirring for 2 h. In order to ensure its complete hydrolysis reaction, a diluted NH_4OH aqueous solution (10%) was added dropwise into transparent $TiCl_4$ aqueous solution to obtain a white precipitate, giving an ultimate suspension of pH 10. In order to remove residual NH_4^+ and Cl^- ions, the precipitate was adequately wished with deionized water till the pH value of filtrated water was below 7.5. Then, the acquired amorphous TiO_2 was well dispersed into water and added with nitric acid solution (20%) in corresponding amount as a peptization catalyst and phase-transfer accelerant. The above suspension was adjusted to pH 1.5 and stirred for 4 h at room temperature, then peptized at 62 °C for 12 h under ultrasonic condition. Finally, pure TiO_2 sol was formed with uniform, stable, and semitransparent

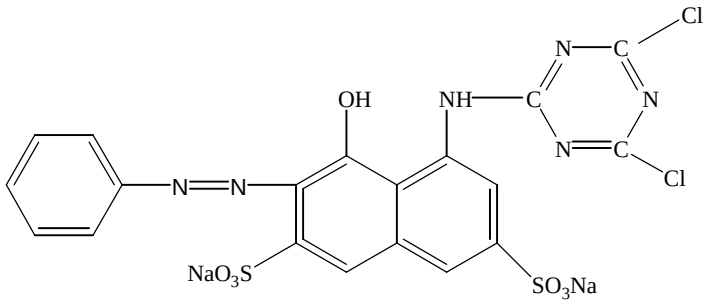

Fig. 1. Molecule structure of dye X-3B (chemical formula = $C_{19}H_{10}O_7N_6C_{l2}S_2Na_2$).

characteristics. The obtained sol can maintain homogenous distribution for quite a long time without sedimentation and delamination phenomena.

2.3. Instruments and analysis methods

The particulate morphology of TiO_2 photocatalysts was observed on atom force microscope (Nanoscope III System, American Digital Corporation, USA). The phase structure of samples were identified by X-ray diffractometer (XD-3A, Shimadazu Corporation, Japan) using graphite monochromatic copper radiation (Cu Kα) at 40 kV, 40 mA over the 2θ range 10–90°. Concentration of X-3B was measured by UV-Vis recording spectro-photometer (UV-2201, Shimadazu Corporation, Japan). The pH value was controlled by acidimeter (pHS-2, Shanghai Rex Instruments Factory). The illuminating light source was cold light source (LGY-150, 150 kW, halogen–tungsten lamp with UV and IR cut-off filter), which mainly emits visible light in the range of 400–800 nm. And the main wavelength is about 550 nm, which is quite matchable to the maximum absorbance of X-3B. All electrochemical experiments were carried out on an electrochemical workstation (CHI-660, CH Instruments Inc., USA).

2.4. Photocatalytic & photoelectrochemical experiments

The experiment of photocatalytic reaction was conducted in a cubage 40 ml, cylindrical silica vessel. TiO_2 sol was acted as photocatalyst and visible light as illuminating light source. And P25 TiO_2 powder as a standard photocatalyst was also applied in the photoreaction experiments in order to compare the photoactivity of TiO_2 sol. Reaction systems were setup by adding TiO_2 sol or P25 TiO_2 powder (adding amount equivalent to 0.1 wt.% TiO_2 concentration) into 20 ml, 100 mg l^{-1} X-3B aqueous solution. Prior to photocatalytic reaction, the hydrosol or suspension system with X-3B and photocatalysts was magnetically stirred in a dark condition for 30 min to establish a adsorption–desorption equilibrium. The aqueous reactants mixture was vertically irradiated under the visible light with constant stirring speed at room temperature. The photodegraded product was collected every 15 min photocatalysis. And X-3B/P25 TiO_2 suspension sample was filtered through two layers of Millipore 0.22 μm films before spectrum analysis. The concentration of X-3B was monitored by measuring characteristic absorbance intensity of X-3B.

The photoelectrochemical property of TiO_2 sol/X-3B was also investigated. The measurements were carried out by using a standard three-electrode system equipped with a quartz window, a saturated calomel reference electrode (SCE) and a platinum plate counter-electrode (CE) placed in the same cell, And optically transparent In_2O_3–SnO_2 oxide conductive glass sheet was selected as working electrode. The electrolyte was 1.0 g l^{-1} TiO_2/100 mg l^{-1} X-3B aqueous mixture with pH 3.5. The working electrode was illuminated from the front side. The photocurrent–time (I–t) measurement was recorded on an electrochemical workstation.

3. Results and discussion

3.1. AFM analysis

The particle morphology and size were investigated by AFM. The samples were prepared on a silica glass sheet by means of spin-coating.

AFM micrograph shows that the TiO_2 sol particles had spheroidal shape and were uniformly spread out on the support. There did not appear any obvious particles agglomeration. The average size was about 25 nm for TiO_2 sol particles (Fig. 2a). However, compositive single nanoparticle of P25 TiO_2 was about 45 nm. And these particles in colloidal suspension obviously tended to aggregate and finally had formed congeries with hundreds nanometer in size (Fig. 2b).

3.2. XRD analysis

Regarding the titania phase character, amorphous TiO_2 seldom displayed photocatalytic activity due to some non-bridging oxygen (NBO) in bulk TiO_2 as defects. And so, crystal structure of TiO_2 sample greatly affects the photoactivity. The phase state of TiO_2 sol was investigated by XRD (Fig. 3).

In comparison with the XRD pattern of the standard anatase crystalline TiO_2, the prepared TiO_2 sol particles had already formed anatase crystal structure due to the presence of attributive peaks (2θ = 25.4,

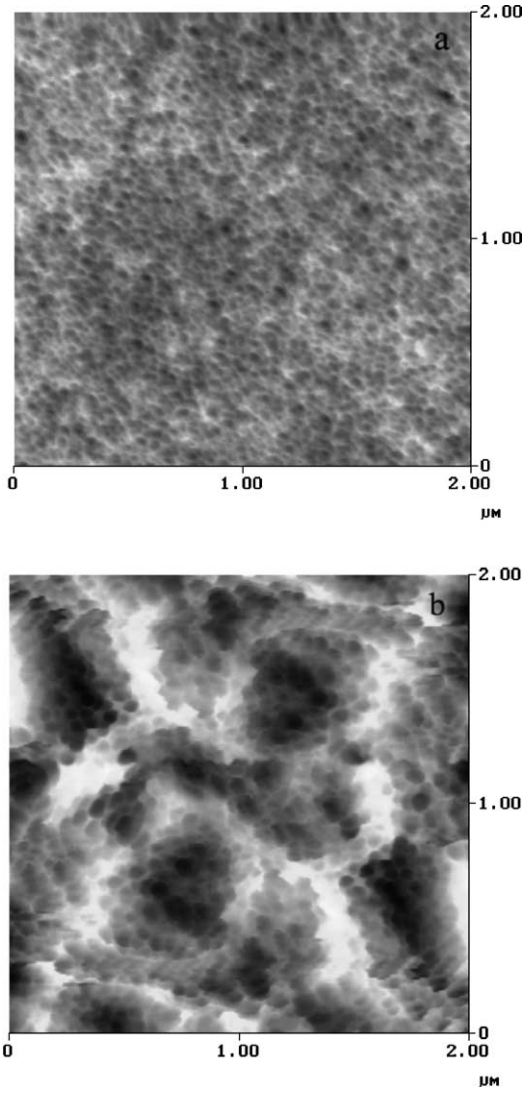

Fig. 2. AFM micrographs of (a) TiO_2 sol particles (b) P25 TiO_2 powder particles. The x–y axis is scaled in micrometers (μm).

38.0, 47.8, and 54.6°) (Fig. 3). It means that phase transformation from amorphous to anatase structure, which requires commonly high temperature calcination at least 400 °C, can be achieved by digesting and peptizing treatment of TiO_2 sol at moderate preparation condition [7]. Very broad diffraction peak at 1 0 1 plane ($2\theta = 25.4°$) was due to its small crystallite size of TiO_2 sol particles. TiO_2 sol sample did not appear any other diffraction peaks of new crystal phase apart from anatase. The crystal structure of TiO_2 particles was the prerequisite for acting as photocatalysts.

The mean size of the single crystallite can also be determined from full-width at half-maxima (FWHM) of corresponding X-ray diffraction peaks by using Scherrer's formula $D = (K\lambda)/(\beta \cos\theta)$, where λ is the wavelength of the X-ray radiation ($\lambda = 0.15418$ nm), K the Scherrer constant ($K = 0.9$), θ the characteristic X-ray diffraction peak ($\theta = 12.7°$) and β is the full-width-at-half-maximum of the (1 0 1) plane (in radians). The estimated nanocrystallites size of TiO_2 sol sample was 2.25 nm.

3.3. PSD analysis

The particles in the TiO_2 sol system seldom have the same size and their size may vary over quite a wide range [8]. The average particle size and particle size distribution (PSD) can be determined by light-scattering size analyzers.

Fig. 4 shows that TiO_2 sol particles had single-modal distribution characteristic and particle size distributes from 14 to 35 nm with the maximum peak at 21 nm. However, P25 TiO_2 particles in aqueous suspension obviously increased in size and distributed from 148 to 208 nm with the maximum peak at 174 nm. By comparison, TiO_2 sol particles displayed a narrow distribution characterization with small particle size (mean size 21 nm). However, P25 TiO_2 particles showed a broad distribution characterization (mean size 174 nm). PSD measurement result of TiO_2 sol particles was in good agreement with the measured size by AFM (25 nm), but far different from the estimated size by XRD method. Twenty-one nanometers was the mean size of dispersed TiO_2 sol particle by PSD analysis method and 2.25 nm was the estimated size of TiO_2 sol particle single crystallite by XRD analysis method. However, P25 TiO_2 particles in the aqueous medium had obvious tendency to aggregate and many individual nanoparticles eventually formed big particles aggregation as shown in above AFM image.

3.4. Adsorption behavior

The heterogenous photocatalytic reaction occurred mainly at the interface of reactants/photocatalysts. Thus, the affinity property between them plays an important role on overall reaction rate [9]. The effect

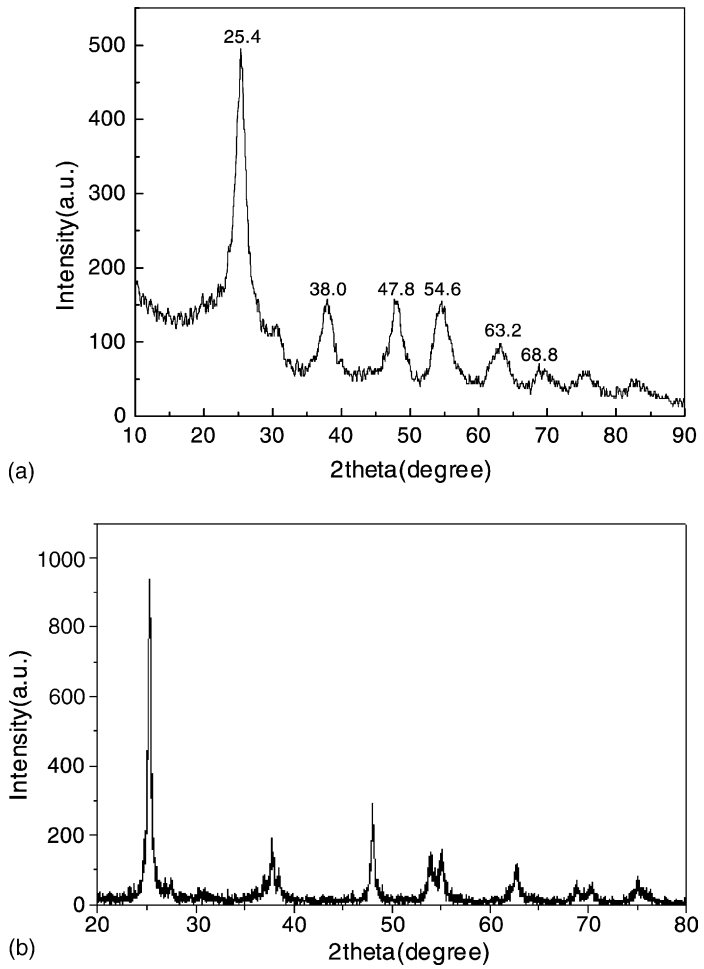

Fig. 3. XRD patterns of (a) TiO_2 sol particles and (b) the standard anatase crystalline TiO_2.

of adsorption–desorption equilibrium was investigated between X-3B and TiO_2 in aqueous medium after 30 min adsorption in darkness. The interfacial adsorption effect of X-3B/TiO_2 was shown in Fig. 5.

Fig. 5 shows that adsorption amount of X-3B rose with the increase of photocatalyst concentration in bulk solution. At the same condition, TiO_2 sol particles obviously possessed better adsorption capability to X-3B than P25 TiO_2 powder. In suspension system, X-3B adsorption amount by P25 TiO_2 was linearly augmented when P25 TiO_2 concentration increased from 0 to 2.0 mg l^{-1}. However, in the sol system, X-3B adsorption amount by TiO_2 sol rapidly increased when TiO_2 sol concentration increased from 0 to 1.0 mg l^{-1}. And TiO_2 sol particles reached saturation adsorption when its concentration was about 1.0 mg l^{-1}. Particles size and adsorption system should be the key factors in affecting adsorption property. Moreover, severe particles aggregation in P25 TiO_2 suspension system also greatly weakened the adsorption capability of TiO_2 particles.

3.5. Photoelectrochemistry property

The photoactivity of dye sensitized TiO_2 greatly depends on the efficiency of electron excitation, electron–cation radicals pairs separation and charge transfer [10,11]. In order to investigate the interfacial electron transfer between TiO_2 particles and charge carriers, photoelectrochemical experiment was carried

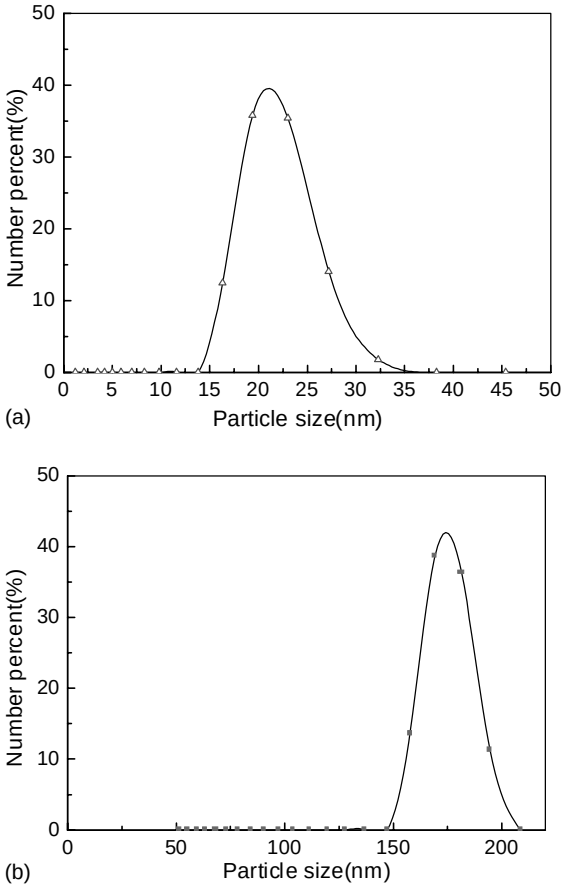

Fig. 4. PSD of (a) TiO_2 sol particles in hydrosol and (b) P25 TiO_2 particles in aqueous suspension. TiO_2 concentration: $1.0\,g\,l^{-1}$.

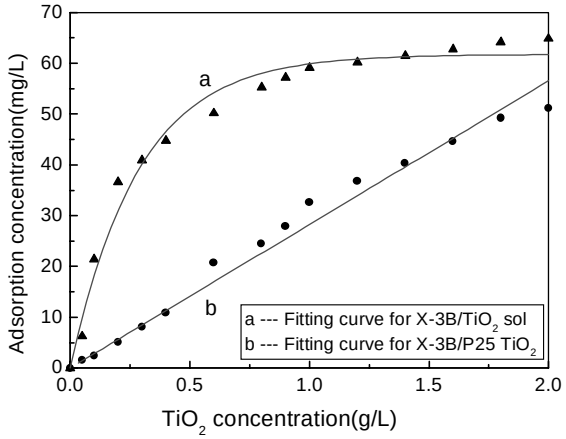

Fig. 5. Adsorption concentration of X-3B (c_a) in terms of TiO_2 photocatalyst concentration (c_p). (a) (▲) X-3B/TiO_2 sol supernate by centrifugation treatment, curve fitting formula $c_a = 61.72[1-\exp(-3.50c_p)]$, correlation coefficient $R = 0.9916$; (b) (●) X-3B/P25 TiO_2 supernate by centrifugation treatment, $c_a = 28.26c_p$, correlation coefficient $R = 0.9895$; initial X-3B concentration: $100\,mg\,l^{-1}$.

out. The working electrode potential was located at 0 V in order to simulate the same working condition as photocatalysis of the dye/TiO_2 reaction system in bulk solution. The photocurrent–time (I–t) profiles without any bias electrode potential were shown in Fig. 6.

Without visible light irradiation, the photocurrent was located at 0.1 μV as darkness current. The photocurrent was rapidly generated at the beginning of illumination, and soon increased to a steady value with instant illumination time. Once light-off, photocurrent rapidly fell down to the initial value. There was no decay of the photocurrent and no downward peak under the light-on condition because of the fast transfer of electrons through out-circuit. The current was stable on the interval time (20 s) of the pulsed visible light irradiation. However, photocurrent intensity of X-3B/TiO_2 hydrosol system (0.60 μA) was stronger than that of X-3B/P25 TiO_2 suspension system (0.42 μA). The photocurrent intensity mainly depended on electron generation capacity and electron transfer effectiveness between X-3B/TiO_2 nanoparticles and working electrode. The X-3B dye sensitization process involved the excitation of dye molecules by absorbing visible light photons and

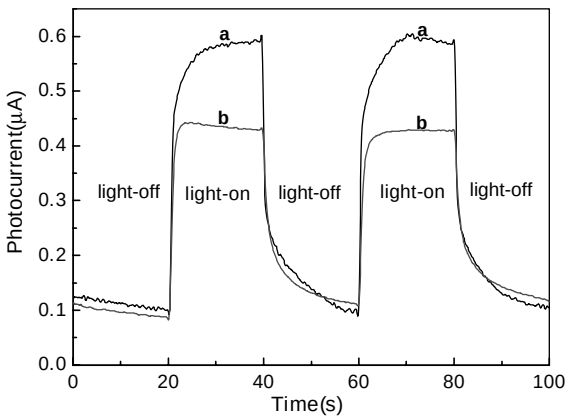

Fig. 6. Photocurrent of (a) X-3B/TiO_2 hydrosol (b) X-3B/P25 TiO_2 suspension system in terms of visible light irradiation.

subsequent electron injection from the excited state of dye to TiO_2 conduction band (CB). Then the electrons underwent transfer process from CB to conductive film of working electrode and finally formed out-circuit. In this process, TiO_2 particles acted as a bridge connecting dye X-3B and working electrode. The difference in photocurrent at light-on condition resulted from different electron transfer efficiency of two kinds of X-3B/TiO_2 reaction systems. So, better X-3B adsorption effect of TiO_2 sol nanoparticle might make great contribution to the higher photocurrent.

3.6. Photocatalytic activity

The photocatalytic activity of TiO_2 sol was characterized by the degradation experiment of X-3B dye as a probe molecule. UV-Vis absorption spectra of X-3B from X-3B/TiO_2 hydrosol and X-3B/P25 TiO_2 suspension system was measured every 15 min following the visible light photocatalysis. All X-3B/TiO_2 sol samples were directly measured by photometer and X-3B/P25 TiO_2 samples were filtered through two layers 220 nm millipore films before measurement by photometer. Fig. 7 shows the changes of X-3B spectra with the same irradiation time intervals (15 min) in the different photocatalyst/X-3B system. And Fig. 8 shows the decrease of X-3B concentration in dependence on visible light irradiation time by different photocatalysts.

Experimental results show that X-3B concentration in these two kinds of X-3B/photocatalyst reaction system both decreased with the visible light illumination, which was in good agreement with the degressive tendency of UV-Vis characteristic absorption spectra at 512–540 nm. The X-3B degradation reaction can be conducted by P25 TiO_2 powder in suspension system as well as by TiO_2 sol in hydrosol reaction system. The difference in initial X-3B concentration in Fig. 8 was due to the different X-3B adsorption effects by two sorts of photocatalysts. By comparison with declining slope of X-3B degradation curves, both TiO_2 sol particles and P25 TiO_2 powder have similar photocatalytic capability. After 180 min photocatalysis, the X-3B decreased to 13.37 mg l^{-1} for X-3B/TiO_2 sol and 18.13 mg l^{-1} for X-3B/P25 TiO_2 reaction system. The above data mean that TiO_2 sol particles display a little higher photocatalytic efficiency than P25 TiO_2 under the same reaction condition. The difference in photoactivity was due to different crystal structure (prepared TiO_2 sol particles with pure anatase crystalline structure and commercial P25 TiO_2 powder with 80% anatase & 20% rutile crystalline structure) since anatase is usually more active than rutile. Furthermore, the light transmitting condition is another factor to affect the effective absorption of excitation photons. The transparent hydrosol reaction system is good for light transmission due to small sol particle size and well particles distribution. On the contrary, suspension reaction system more likely causes light scattering due to mass particles aggregation.

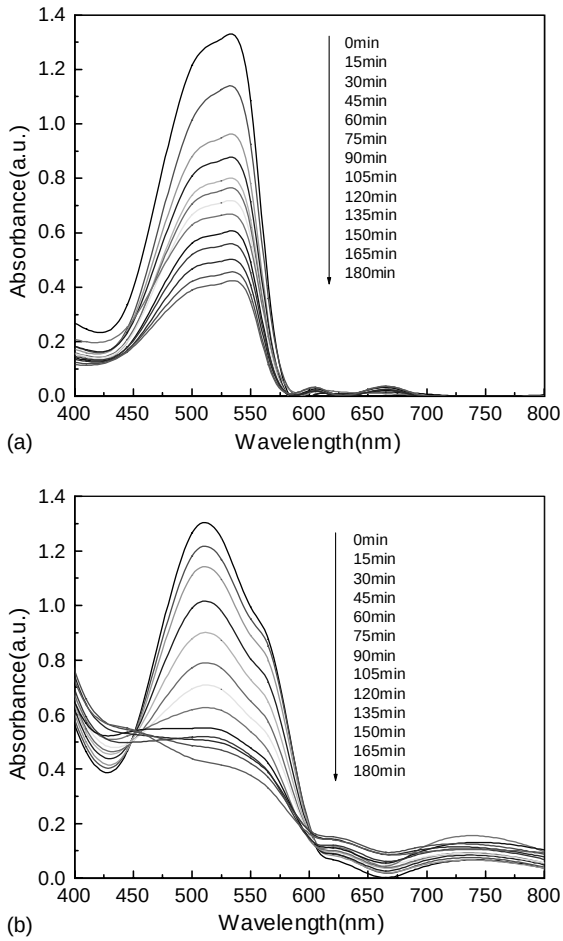

Fig. 7. UV-Vis absorption spectra of photocatalysis samples from (a) X-3B/P25 TiO_2 suspension system and (b) X-3B/TiO_2 hydrosol system under visible light irradiation (original X-3B: 100 mg l^{-1}; photocatalyst: 1.0 g l^{-1}; initial X-3B/photocatalyst mixture through 30 min adsorption process in darkness).

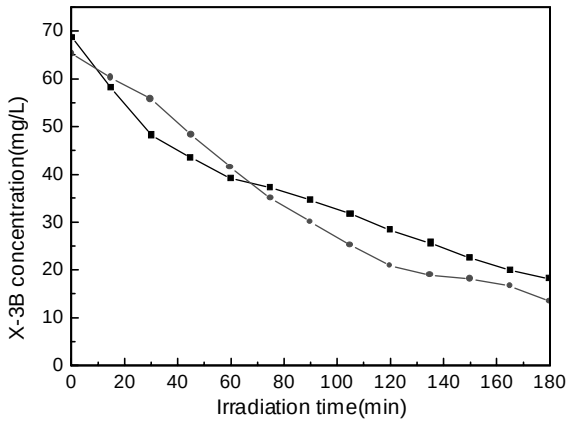

Fig. 8. X-3B concentration(c) as function of visible light irradiation time (t). (■) X-3B/P25 TiO_2 suspension reaction system; (●) X-3B/TiO_2 hydrosol reaction system.

The sensitized photocatalysis mechanism is very different from direct photocatalysis mechanism, which is involved in electron–hole pair separation for TiO_2 semiconductor [12]. In the process of sensitized photocatalysis, the electron is normally injected from excited dye molecule (dye*) to CB of TiO_2, then trapped by electron scavenger (oxygen molecule). The cation radical ($dye^{\bullet+}$) produced by charge injection is less stable than the ground state of the compound. And it is also extremely susceptible for the cation radical and the electron to recombine if the injected electrons accumulate in the conduction band. So, electrons transfer and electrons trapping are key steps to inhibit electron–cation radical recombination.

By comparison, the electron transfer route in sensitized photocatalysis was very similar to that in photoelectrochemical process (from excitated dye molecule (dye*) to CB of TiO_2, then terminated at conductive film. The photoelectrochemical data mentioned above reveal that X-3B/TiO_2 sol system showed stronger photocurrent than X-3B/P25 TiO_2 suspension system. The better electrons transfer between X-3B and TiO_2 sol nanoparticles leads to more effective electron–cation radical separation of excitated X-3B (dye*). And so, more cation radicals could undergo quick degradation to yield stable products, which was reflected in the superior photoactivity of TiO_2 sol:

$$dye^{\bullet+} \rightarrow \text{products} \quad \text{and} \quad dye^{\bullet+} + O_2{}^{\bullet-} \rightarrow \text{products}$$

The advantage of sensitized photocatalysis is that the range of excitation energies is extended into the visible region, as in the present case, making the use of solar light for destruction of non-biodegradable textile and dyestuff wastewaters more efficient.

3.7. Recycle use and photoactivity

The regeneration of TiO_2 photocatalyst was one of key steps to making heterogeneous photocatalysis technology for practical applications [13]. Recycle use of TiO_2 sol photocatalyst was designed and photocatalytic reaction was carried out as the following. TiO_2 sol was sensitized to pH value in aqueous medium. TiO_2 sol can appear flocculation when pH value was adjusted to above 9.0. And the obtained flocculation can be prepared into sol particles again when pH value was adjusted to below 4.0 with fully stirring and ultrasonic agitation treatment. According to this characteristic, recycle experiment of the photocatalytic decomposition of X-3B on TiO_2 sol was designed in order to examine the photoactivity of TiO_2 sol after being reused. The mixture of X-3B and TiO_2 sol after 2 h photocatalysis was adjusted to 10.0 with 10 wt.% $NH_3{\cdot}H_2O$ solution. After removal of transparent supernate, the deposited flocculation was well dispersed into semitransparent TiO_2 sol system through adequately stirring while pH value was adjusted to 3.0 with HCl (1.0 mol l^{-1}). The above process was repeated so as to reuse the same TiO_2 sol photocatalyst. Fig. 9 shows UV-Vis spectra of obtained supernate after photocatalytic reaction of X-3B/TiO_2 sol system for different reusing time. The original supernate was directly measured by photometer without further filtering treatment.

Fig. 9 shows that the characteristic absorption peaks (512–540 nm) of X-3B in supernate completely disappeared through TiO_2 sol photocatalytic degradation reaction for four times recycle use. The weak adsorption peaks of sample after photocatalysis by the fifth reused TiO_2 sol means photoactivity of TiO_2 sol had a little decline.

The photodegradation effect by reusing TiO_2 sol photocatalyst was evaluated by comparing residual X-3B concentration in the supernate (Fig. 10).

Fig. 10 shows the TiO_2 sol almost kept the same photocatalytic activity after three times reuse (X-3B degradation efficiency above 97%). Even after five

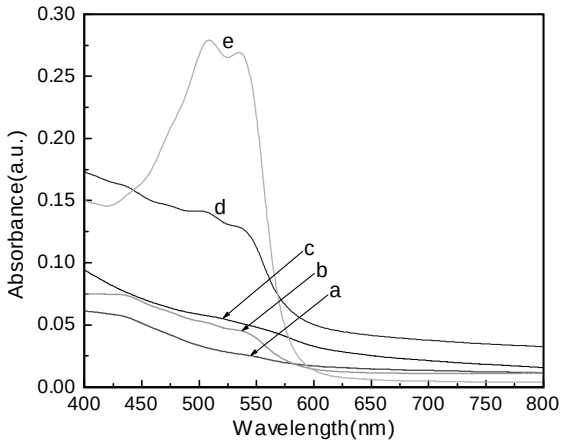

Fig. 9. UV-Vis absorption spectra of supernate separated from X-3B/TiO_2 hydrosol system after 120 min photocatalysis for different reusing time. (a) First use, (b) second use, (c) third use, (d) fourth use, (e) fifth use.

times reuse, X-3B degradation efficiency by TiO_2 sol was above 84%. This result means that TiO_2 sol can act as a useful photocatalyst to drive photodegradation reaction. Most importantly, TiO_2 sol can be reused for several times without great decrease in photoactivity during the photocatalytic reaction. TiO_2 sol photocatalyst, as a novel catalyst, exhibits potential application on industrial area although it still needs to improve reusing times meanwhile keeping high photoactivity.

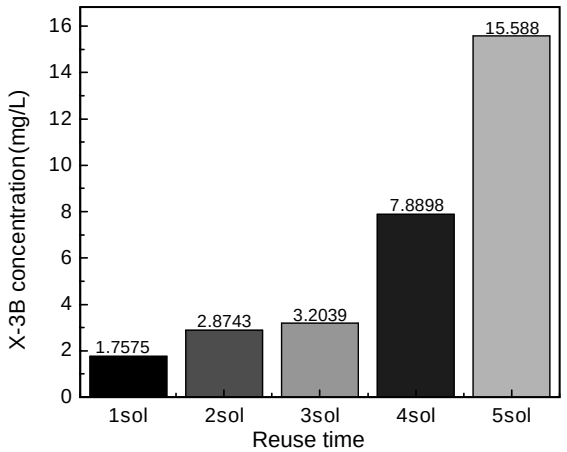

Fig. 10. Concentration of residual X-3B in supernate after TiO_2 sol photocatalysis for different reusing times. Initial concentration: 100 mg l^{-1}; TiO_2 sol: 1.0 g l^{-1}; reaction time: 120 min.

4. Conclusion

TiO_2 sol was studied on the photocatalytic activity. A novel hydrosol reaction system was designed to photodegrade dye X-3B. The results proved that as-prepared TiO_2 sol particles without calcination treatment had anatase crystal structure and narrow particles size distribution characteristics. TiO_2 sol can act as a photocatalyst and effectively photodegrade dye X-3B under visible light illumination by sensitized photocatalysis reaction mechanism. Good adsorption property and anatase crystal structure of TiO_2 sol particles great contributed its high photocatalytic activity and photocurrent response. By taking advantage of sensitiveness to the pH value, TiO_2 sol can be applied to recycle use in photocatalytic reaction while keeping high photoactivity. This characteristic is very different from P25 TiO_2 powder in respects of reaction system and catalyst types.

Acknowledgements

This work was financially supported by the Hi-Tech Research and Development Program (863 Program) of China (No. 2002AA302304) and the National Natural Science Foundation of China (No. 60121101).

References

[1] A. Fujishima, T. Rao, A.D. Tryk, J. Photochem. Photobiol. C 1 (2000) 1.
[2] K. Yogo, M. Ishikawa, Catal. Surv. Jpn. 4 (2000) 83.
[3] R. Andreozzi, V. Caprio, A. Insola, R. Marotta, Catal. Today 53 (1999) 51.
[4] V. Vamathevan, H. Tse, R. Amal, G. Low, S. McEvoy, Catal. Today 68 (2001) 201.
[5] A. Di Paola, E. García-López, S. Ikeda, G. Marcì, B. Ohtani, L. Palmisano, Catal. Today 75 (2002) 87.
[6] A.P. Xagas, M.C. Bernard, G.A. Hugot-Le, N. Spyrellis, Z. Loizos, P. Falaras, J. Photochem. Photobiol. A 132 (2000) 115.
[7] L. Znaidi, R. Séraphimova, J.F. Bocquet, C. Colbeau-Justin, C. Pommier, Mater. Res. Bull. 36 (2001) 811.
[8] E. Reverchon, P.G. Della, D. Sannino, P. Ciambelli, Powder Technol. 102 (1999) 127.

[9] M.S. Chiou, H.Y. Li, Chemosphere 50 (2003) 1095.
[10] H. Hidaka, K. Ajisaka, S. Horikoshi, T. Oyamab, K. Takeuchi, J. Zhao, N. Serpone, J. Photochem. Photobiol. A 138 (2001) 185.
[11] J.A. Byrne, B.R. Eggins, J. Electroanal. Chem. 457 (1998) 61.
[12] A. Castellan, D.S. Perez, A. Nourmamode, S. Grelier, M.G.H. Terrones, A.E.H. Machado, R. Ruggiero, J. Braz. Chem. Soc. 10 (1999) 197.
[13] R.D. Sun, A. Nakajima, T. Watanabe, K. Hashimoto, J. Photochem. Photobiol. A 154 (2003) 203.